Nanoparticulated Gold: Syntheses, Structures, Electronics, and Reactivities

Günter Schmid*[a] and Benedetto Corain[b]

Keywords: Gold / Nanoparticles / Synthetic methods / Quantum dots / Self-assembly / Heterogeneous catalysis

This microreview deals mainly with the synthesis and the electronic and chemical properties of gold nanoparticles. Modern synthetic routes, based on physical and on chemical procedures, as well as structural and optical features, are described. The bulk-to-molecule transition is discussed by studying size-controlled quantum-size effects, resulting in the determination of discrete electronic energy levels in Au_{55} clusters. Conductivity measurements of three- and two-dimensionally organized ligand-protected Au_{55} clusters are described, as well as the current techniques for the generation of ordered monolayers and artificial patterns of quantum dots. Finally, some aspects of the chemical activity of gold nanoparticles are discussed by considering ligand-exchange processes and, last but not least, the expanding role of gold nanoparticles in catalysis is considered.

1. Introduction

Gold: quintessence of beauty and nobility among the metals. Some time during the Stone Age man discovered and learned to appreciate gold not only for its beauty but also for its resistivity against corrosion. Moreover, because of its relative scarcity, gold has been considered a substance of great value over millennia and today it still serves as monetary parity in many countries. The Old Testament is full of stories dealing with gold and numerous wars have been started because of gold. The early historical use of gold has also to do with its natural deposits as nuggets, which meant that no chemical processes were needed to be able to use it. Due to its softness it could be hammered into articles of jewellery even in ancient times. Numerous civilizations therefore had already started gold mining by at least the 4th millennium BC. However, the mines operated by the Egyptians in Nubia surpassed all of them by far. Gold became a decisive reason for the power of the Egyptian rulers. It was, and still is, synonymous of wealth.

In contrast to the long history of gold, the development of its chemistry was retarded because of its noble character. It can only be dissolved in oxidising media like aqua regia or by complexing species such as cyanides under air. Nowadays, the chemistry of gold is rather broad, beginning with classical complex chemistry via novel organometallic chemistry up to solid-state chemistry where so-called aurides give evidence of the high electronegativity of this unique metal.

Long before the development of modern gold chemistry the special appearance of gold was appreciated by mankind: its ruby red colloids were used to color glasses and cer-

[a] Universität Duisburg-Essen,
Universitätsstrasse 5−7, 45117 Essen, Germany
E-mail: guenter.schmid@uni-essen.de
[b] Università di Padova, Dipartimento di Chimica Inorganica, Metallorganica ed Analitica,
Via Marzolo 1, 35131 Padova, Italy

Günter Schmid studied chemistry at the University of Munich. He received his Diploma in 1962 and his Doctor's Degree in Inorganic Chemistry in 1965, both at the University of Munich. In 1966 he moved to the University of Marburg, Germany, and finished his Habilitation in 1969. In 1971 he got a professorship at the University of Marburg and he then moved to the University of Essen, Germany, where he became the director of the Institute for Inorganic Chemistry (1977). His main research interests include the synthesis and investigation of large transition metal clusters and colloids, the generation of three-, two- and one-dimensional arrangements of quantum dots, and heterogeneous catalysis.

Benedetto Corain graduated in Chemistry at the University of Padova in 1965. After serving as Assistant Professor and Associate Professor in Padova, he moved to the University of L'Aquila in 1993 as full Professor of Chemistry and he was called back with the same status from his previous University in 1999 (Faculty of Sciences). He spent one year as a Research Assistant at the Department of Chemistry, Imperial College, London in 1966 and as a Visiting Professor (Humboldt fellow) at TU Munich in 1981 and 1998 and at the University of Essen in 2002. His present research interests include basic and applied metal coordination chemistry and macromolecular chemistry, with particular emphasis on reactive and functional cross-linked polymers as supports for metal nanoclusters.

MICROREVIEWS: This feature introduces the readers to the authors' research through a concise overview of the selected topic. Reference to important work from others in the field is included.

amics. Solutions of colloidal gold were also used as tonics and elixirs, especially in combination with alcohol. Colloidal gold is still applied to treat arthritis.[1]

Scientifically, the beginning of the chemistry of gold colloids dates from the middle of the nineteenth century, when Michael Faraday performed his famous experiments to generate gold colloids.[2] He reduced tetrachloroaurate using white phosphorus to yield deep-red gold sols. At the beginning of the 20th century it was Wilhelm Ostwald who contributed decisively to the further development of colloid science.[3] He was the first to point out that the properties of metal particles in the nanometer range are predominantly determined by surface atoms and he concluded that those nanoparticles, called colloids, should exhibit novel properties with respect to bulk particles. The term "colloid" has meanwhile been mostly substituted by "nanoparticle" or "cluster". Both expressions are not very precise. They simply tell us that a particle consists of an assembly of atoms, from a few up to several hundred thousands or millions, in the size range between 1 and usually not more than 50 nm.

The miniaturization of gold to the nanometer range has dramatic consequences for its physical and chemical properties. (In principle these consequences are also valid for other metals. Gold, however, is an outstanding example.) Two examples shall elucidate the change of bulk properties when the nanosize regime is reached: the melting point and the color. Figure 1 shows the melting points of gold nanoparticles from ca. 20 to 2 nm in diameter.[4]

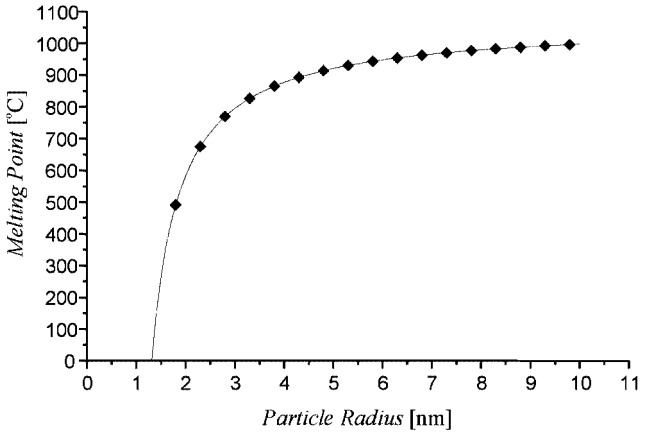

Figure 1. Relationship between particle size and melting point of gold nanoparticles

As we can see, the melting point drops below that of bulk gold (1064 °C) if the particle radius is less than 10 nm. This has to do with the increasing number of surface atoms with decreasing particle size. Surface atoms have lower coordination numbers than inner atoms and therefore become mobile more easily.

Figure 2 shows the typical color of 10 ± 5 nm gold particles.[5] In this particular case the particles are embedded in the pores of a transparent alumina membrane. The reason for the special color of metal nanoparticles is the so-called plasmon resonance, a well understood phenomenon, which is quantitatively described by the Mie theory.[6,7]

Figure 2. Photograph of a nanoporous alumina membrane, filled with 10 ± 5 nm gold nanoparticles

2. Syntheses

The number of procedures for generating gold nanoparticles is almost indeterminable. Most of them have been known for decades. For this reason only some relevant and general synthetic techniques shall be discussed here briefly. Two main routes to gold nanoparticles are available: a physical and a chemical one. Physical methods are defined as those by which gold nanoparticles are directly generated from bulk gold via atoms by various distribution techniques, whereas chemical routes use gold compounds as a starting material, linked with reduction steps.

An important aspect is the stabilization of the particles to avoid coalescence between them. This stabilization can occur in many different ways, for instance by electrostatic repulsion, steric hindrance, ligand molecules or embedding in nanocapsules such as micelles. Some of these opportunities will be discussed as part of the synthetic routes.

2.1 Physical Methods

Metal vapours usually consist of atoms. The simplest way of obtaining nanoparticles is therefore the generation of metal atoms in the gas phase followed by their controlled condensation to nanoparticles. This is the well-known metal-vapour synthesis.[8] In special cases the colloidal metals can be studied in the gas phase; however, in order to obtain them as matter, the vapours have to be condensed into a dispersing medium. Numerous modifications of this established technique have been successfully applied in the past[9] and will not be repeated in this article. Only some more recent and promising results shall be discussed.

Laser ablation methods have become commonly used techniques.[10–14] However, the size distribution of the resulting particles is usually rather broad. Improvements were obtained by the so-called "laser-induced size reduction". This is based on the well expressed plasmon resonance of

gold nanoparticles around 520 nm and was used to change the size and geometry of the particles.[15−20] Very narrowly distributed gold nanoparticles with a diameter of 1.7 and 3.4 nm were obtained with a 532 nm pulsed laser irradiation of gold metal plates in diluted sodium dodecylsulfate solutions.[21]

A gram-scale synthesis of thiol-stabilized gold nanoparticles by solvated metal atom dispersion and digestive ripening was recently reported.[22] The method is based on the so-called solvated metal atom dispersion technique (SMAD). A well-known reactor was used to generate atoms from a piece of bulk gold.[23] The Au atoms were frozen at 77 K in acetone vapour and were then warmed up to give gold colloids, stabilized by acetone molecules. In order to attain further stabilization, they were then reacted with dodecanethiol and this enabled good dispersion in toluene. A dramatic effect on the narrowing of the gold particles was obtained by digestive ripening of the gold-toluene dispersion at 120 °C. Particles of 1−40 nm in size were narrowed down to 4−4.5 nm.

As we shall see from the following examples, wet-chemical routes to generate gold nanoparticles are much more versatile.

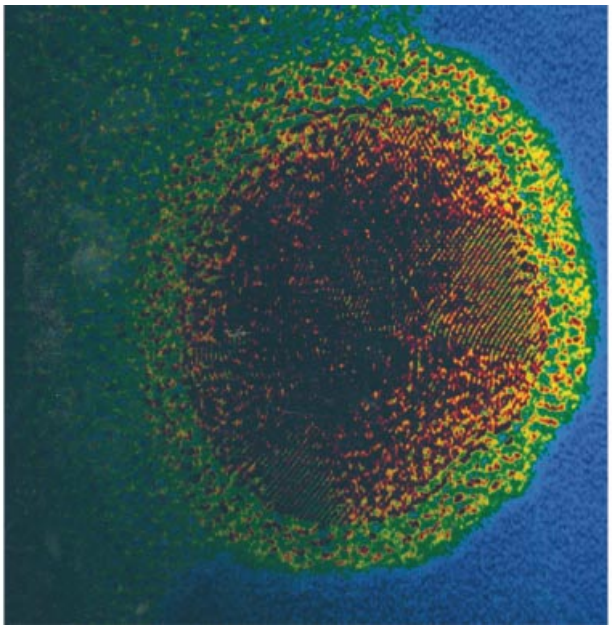

Figure 3. High-resolution transmission electron microscopic (TEM) image of a ligand-protected 11 × 13 nm gold nanoparticle; the polycrystalline gold core and the protecting shell of $P(C_6H_4SO_3Na)_3$ molecules can clearly be distinguished

2.2 Chemical Routes

As already mentioned, Michael Faraday was the first to study the formation of gold sols from a scientific point of view.[2] Phosphorus was the agent he used for the reduction of $[AuCl_4]^-$ ions. In the course of the last century numerous easier to handle reducers were found. A few of the more relevant procedures, especially the newer ones, are mentioned below.

Among the so-called salt reduction methods, the Turkevitch route still is one of the most applied procedures.[24] Sodium citrate reduces $[AuCl_4]^-$ in hot aqueous solution to give colloids of 15−20 nm. Citrate itself and its oxidation products (e.g. acetone dicarboxylate) can act as protecting agents, if no other stabiliser is used.[25,26] Dozens of variations have meanwhile been found. The use of stronger ligands than citrate was a major improvement for the synthesis and handling of gold sols. Phosphanes and thiols turned out to be excellent stabilisers due to rather strong Au−P bonds and even better Au−S bonds. These molecules allow the isolation of gold nanoparticles as solid materials that can be redispersed in appropriate solvents. This is not possible with weakly binding stabilisers such as citrate. Water-soluble phosphanes have been successfully used to shield gold colloids.[27] For instance, $P(C_6H_4SO_3Na)_3$ stabilises gold particles of 15−20 nm to such an extent that they become isolable as golden leaves that can be redispersed in deionized water with the typical purple-red color. Figure 3 shows a TEM image of an individual gold nanoparticle where the envelope of stabilizing phosphanes can be observed.[28]

PPh_3 acts as a rather good ligand for 1.4 nm Au_{55} clusters in $Au_{55}(PPh_3)_{12}Cl_6$. The latter is easily obtained by reduction of Ph_3PAuCl by gaseous B_2H_6 in benzene or toluene at elevated temperatures.[29,30] This compound will be the focus of attention of the following chapters because of its particular electronic properties. It is readily soluble in CH_2Cl_2 however, it can also be transformed into a water-soluble species by exchanging PPh_3 with $Ph_2PC_6H_4SO_3Na$ or $Ph_2PC_6H_4SO_3H$.[31]

Besides phosphanes, thiols are the most important type of stabilizing molecule for gold nanoparticles of any size. It is an accepted assumption that the use of thiols leads to the formation of RS^- thiolates that form strong covalent Au−S bonds. Since they bind more strongly to gold than phosphanes do, phosphanes can usually be substituted by thiols. However, it is also observed that the size of the original gold particles may change during the exchange process.[32,33] $[B_{12}H_{11}SH]^-Na^+$ [34] and SH-functionalized silsesquioxanes such as $(cyclopentyl)_7Si_8O_{12}(CH_2)_3SH$[35] have been successfully applied to remove phosphanes quantitatively from the surface of Au_{55} clusters. The ionic $[B_{12}H_{11}SH]^-Na^+$ transforms the CH_2Cl_2-soluble phosphane-stabilized clusters into water-soluble ones, whereas the alkyl terminated silsesquioxane makes the same particle soluble in apolar solvents such as hexane or pentane.

One of the most popular modern methods for preparing gold nanoparticles of various sizes comes from Brust et al.[36] It uses $NaBH_4$ to reduce gold salts in the presence of alkanethiols to yield gold particles of 1−3 nm. By varying the thiol concentration, the particles sizes can be controlled between 2 and 5 nm.[37] Recently, thiol-stabilized gold nanoparticles have become available following a seeding growth approach starting with 3.5 nm particles. The particle size can be varied by changing the seed-particle-to-metal-salt ratio.[38] Gold nanoparticles in the size range of about 10 to 30 nm or more have been synthesized by the $NaBH_4$

method using mercaptosuccinic acid for stabilization.[39] By varying the succinic-acid-to-$HAuCl_4$ ratio from 2.5 to 0.5, particles of 10.2, 10.8, 12.8, 19.4, and 33.6 nm were isolated as water-redispersable powders.

11-Mercaptoundecanoic acid was also used to cover gold nanoparticles generated by the Brust method.[40] The carboxylic functions were then treated with trifluoroacetic anhydride to give the corresponding carboxylic anhydrides which are highly reactive and can, for instance, be used to anchor the nanoparticles on silica supports.

An elegant and valuable route is the generation of gold nanoparticles inside "nano-reaction vessels". Micelles can be considered appropriate chemical reactors. Due to their limited size, the control of growth by ligand concentration or other experimental conditions is not required. Möller et al. contributed decisively to this modern field of nanoscience. They used diblock co-polymers exhibiting regularly organized micelles into which tetrachloroaurates were transported, followed by a reductive step with hydrazine or $NaBH_4$ and formation of the nanoparticles.[41−45] Figure 4 shows one of those nanoparticle arrangements in a diblock co-polymer.

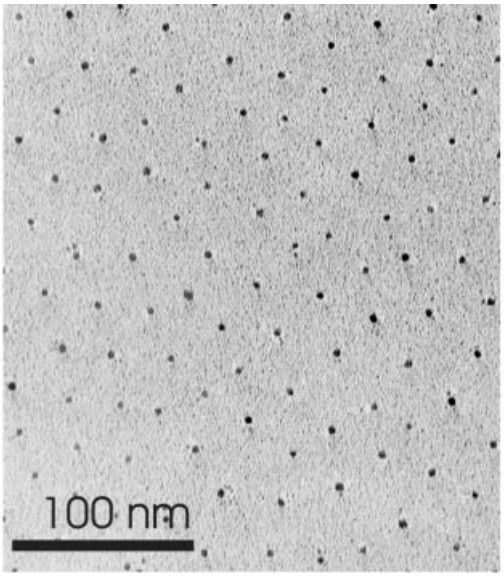

Figure 4. TEM image of 4 nm gold particles in micelles of diblock co-polymers

It must be stated that the above-mentioned examples of synthetic strategies for generating gold nanoparticles are very incomplete. A full overview of all known synthesis techniques would exceed this microreview by far. The purpose of this article is simply to report some novel improvements of well-known methods. We can conclude that since Faraday's time the syntheses have been improved, especially with respect to a better control of the particles size, however, the chemical principles are still just the same: it is the facile reduction of Au^{III} or Au^{I}. Amongst all transition metals, gold is the most electronegative one and consequently it can be generated from its salts by a huge number of reducing species. Not only classical reducers such as hydrides, hydrogen, hydrazine, hydroxylamine, alcohols etc. can be used, but any kind of organic species with some reducing character is suited to produce gold nanoparticles from salts. A so-called "green chemistry" has evolved in recent years, meaning that gold nanoparticles can be generated by natural organic materials via reduction.[46,47] Even different types of fungi have been found to work up gold salts into elemental gold.[48]

3. Structures and Optics

Transmission electron microscopy (TEM) is by far the most valuable tool for studying particle size, distribution, and structure. From thousands of TEM investigations we know that gold nanoparticles exhibit either a mono- or a polycrystalline structure of hexagonal close-packed (hcp) atoms, just like in the bulk state. Even bimetallic core-shell-structured nanoparticles can be identified by various imaging contrasts and by Energy Dispersive X-ray Analysis (EDX) of individual particles.[49,50] An example with a ca. 20 nm gold core and a palladium shell is shown in Figure 5.

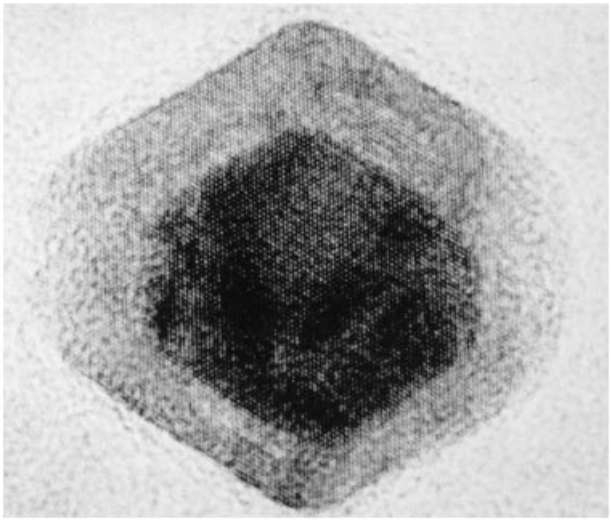

Figure 5. TEM image of a monocrystalline core-shell-structured gold-palladium particle

The smallest particle in this sense is ligand-stabilized Au_{55} which has been investigated not only by TEM, but, for instance, also by X-ray diffraction, EXAFS and Mössbauer spectroscopy. All results indicate an hcp structure.[29,51−55] However, there is an interesting transition with respect to the development of bulk structures. The smallest ligand-stabilized, so-called full-shell cluster, consists of only one central and 12 gold atoms in a first shell (Au_{13}). These have been shown to build up icosahedra.[56,57] An Au_{39} cluster has also been characterized by X-ray diffraction. It consists of a distorted hexagonal close-packed core, protected by 14 PPh_3 and 6 Cl ligands, indicating the transition to bulk structure.[58] Finally $Au_{55}(PPh_3)_{12}Cl_6$ fully reached the bulk structure. These three examples illustrate the development of the bulk state from a molecular level. However, it should

be emphasized that these findings are only valid for ligand-stabilized particles. Conclusions on the situation in bare clusters are not possible.

A characteristic of all gold colloids is the color which can vary between light red via purple-red to bluish-red. This effect is caused by a plasmon resonance, quantitatively described by the Mie theory, as already mentioned. The plasmon resonance is initiated by the interaction of the electric field of visible light with the confined electron-gas of the particle. The wavelength, in the case of gold usually in the region of 500−600 nm, depends on the size of the particle and on the shape and the dielectric properties of the surrounding medium. These facts are quite well understood and will not be discussed here. However, a recent result shall briefly be mentioned, since it shows not only the influence of the particle size on the plasmon resonance, but also on the particles' arrangement and the nature of the surrounding medium.[59] For that purpose nanoporous alumina was filled with various gold nanoparticles. Owing to its transparency, alumina is ideally suited to study the optical properties of nanosized particles inside its pores.[60] Two approaches for placing gold nanoparticles in nanopores are available: the thermal decomposition of $Au_{55}(PPh_3)_{12}Cl_6$ clusters inside the pores to generate larger particles and the use of preformed particles to be filled into the pores by vacuum induction of solutions. An example of a membrane prepared in this manner has already been shown in Figure 2.

As expected, the size of the gold nanoparticles increases with increasing decomposition-temperature, due to the increasing melting point of larger particles (see Figure 1). In the temperature range of 100−800 °C particles with diameters of 4.5 up to 11 nm were observed in sectioned membranes by means of TEM. For example, Figure 6 shows the extinction spectra of a composite consisting of 4.5 ± 1.4 nm particles in 50 nm pores in two different media, namely in air and in toluene.

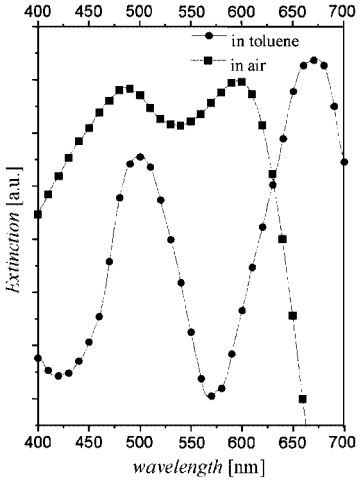

Figure 6. UV/Vis extinction spectra of 4.5 ± 1.4 nm gold nanoparticles in 50 nm alumina pores in air and in toluene, respectively

In air, two absorption peaks are observed at 480 and 600 nm. The low-energy absorbance is probably caused by the excitation of the plasmon resonance along the axis of the wire-like arranged particles. This effect can be seen even by the naked eye: when viewed perpendicularly to the membrane's surface the color is deep red (Figure 2), whereas the edge of the membrane looks blue. On immersing the sample in toluene, not only does the intensity of the peaks increase, but both peaks are red-shifted to 500 and 675 nm, respectively. This red-shift is caused by the change in the refractive index from air to toluene, whereas the increase in intensity comes from the reduction of scattering effects, since toluene has almost the same refractive index as alumina.

The use of preformed nanoparticles has the advantage of narrower size distribution and allows one to observe changes by repeated filling. If 50 nm pores are filled once with 15 nm gold colloids, only one plasmon resonance peak at 525 nm is observed because of the lack of wire-like arrangements. Repeated filling broadens out and shifts the signal to 580 and 590 nm, indicating initial formation of wire-like arrangements. Additional effects have been observed using unpolarised and polarised light with different polarization angles. Theoretical calculations, using the generalized Mie theory,[7,61−63] support the interpretation of the experimental observations.

Plasmon resonance is a size-dependent phenomenon of several metals. Bulk metals reflect light, whereas small molecular clusters do not show any kind of plasmon resonance. This is due to the lack of *quasi* delocalized electrons that are necessary for the interaction with light. On the contrary, the electrons between metal atoms in small clusters are localised. This is known for thousands of oligonuclear organometallic cluster compounds.

A decisive question, which will also be the focus of attention of the following chapters, is: how large or how small should a metal particle be in order for us to observe molecular or metallic properties? In relation to optical properties this question has to be formulated as: when does the plasmon resonance disappear if miniaturization proceeds? In this context, ligand-stabilized Au_{55} clusters play an important role. Ligand-stabilized Au_{13} and Au_{55} clusters were investigated and in both cases the vanishing of the Mie resonance was observed.[64] Again we should remember that the observed effects always include the existence of ligand shells on the particles. In spite of this restriction it can be stated that the 1.4 nm Au_{55} clusters, from an optical point of view, belong rather to the molecular world than to the metallic one. However, we will learn that such statements cannot be generalised, since the method of investigation, temperature and other experimental parameters play a decisive role with respect to what we "see". To conclude these considerations we have to accept that $Au_{55}(PPh_3)_{12}Cl_6$ and its variations do not possess enough mobile electrons to exhibit plasmon resonance. Of course, these findings are related to the special electronic situation in the Au_{55} cluster core. Therefore, the following section will deal exclusively with the electronic properties of this compound.

4. Electronics

4.1 The Quantum Size Effect

In a bulk piece of metal the valence electrons of the participating atoms occupy energy bands instead of discrete levels, as we know from atoms and molecules. In a thought experiment we can proceed with a continuous reduction of dimensions. From a 3D situation with its typical bulk behavior we turn to a film of only a few atoms' thickness (2D). Here, the electrons can only move in two dimensions, whereas in a wire of only a few atoms in diameter, one-dimensionality (1D) of the electronic degree of freedom is enforced. If we cut off a small piece of that wire we reach the zero-dimensional (0D) situation where the remaining electrons are constrained in such a way that they begin to occupy discrete energy levels. A particle of such size no longer follows classical physical laws and has to be described by the quantum mechanical rules used to describe atoms. That is why such pieces of matter are also called "quantum dots" or, with a somewhat more popular expression, "artificial atoms". Pieces of metals following these conditions must exhibit very different physical and chemical properties compared to bulk ones and to typical molecular ones. It was the enormous interest in these novel properties that brought nanoscience to such a level that a wide public, economic and political interest arose. It is the general opinion of experts that nanotechnology will decisively influence man's life in the following century.

Back to the facts, we have to repeat the question we asked in the previous section in a more general way: how many atoms do we need, to cause metallic behavior or how small should a piece of metal be in order to see metallic properties disappearing?

4.2 Physical Tools

There are many physical methods to investigate quantum-size effects. It would exceed this article by far to mention and to discuss all of them, therefore only a few shall be selected to explain what happens when particles size is continuously reduced. It should be mentioned that many of the investigations during the last two decades involved other metals as well as gold, since quantum-size effects can be studied with any kind of metal, and, of course, also with semiconductors. However, gold played once again an important role in the process of our understanding. Some hints have already been given by the optical phenomena discussed in section 3.

One important contribution to this major problem was made by the observation of electron-phonon coupling in gold particles of different size.[65] This relation informs us on the interplay between the rate of energy transfer from electrons to lattice and the number of atoms in the particle. It was found that the electronic relaxation-speed, induced by laser pulses of 200 fs of an energy of 250 μJ/pulse at 780 nm, varies characteristically with the particle size. $Au_{13}(dppm)_6(NO_3)_4$ (dppm = $Ph_2P\text{-}CH_2\text{-}PPh_2$)[56] (core diameter 0.7 nm), $Au_{55}(Ph_2PC_6H_4SO_3Na)_{12}Cl_6$ [31] (core diameter 1.4 nm) and 15 nm colloids were tested. Figure 7 shows the results.

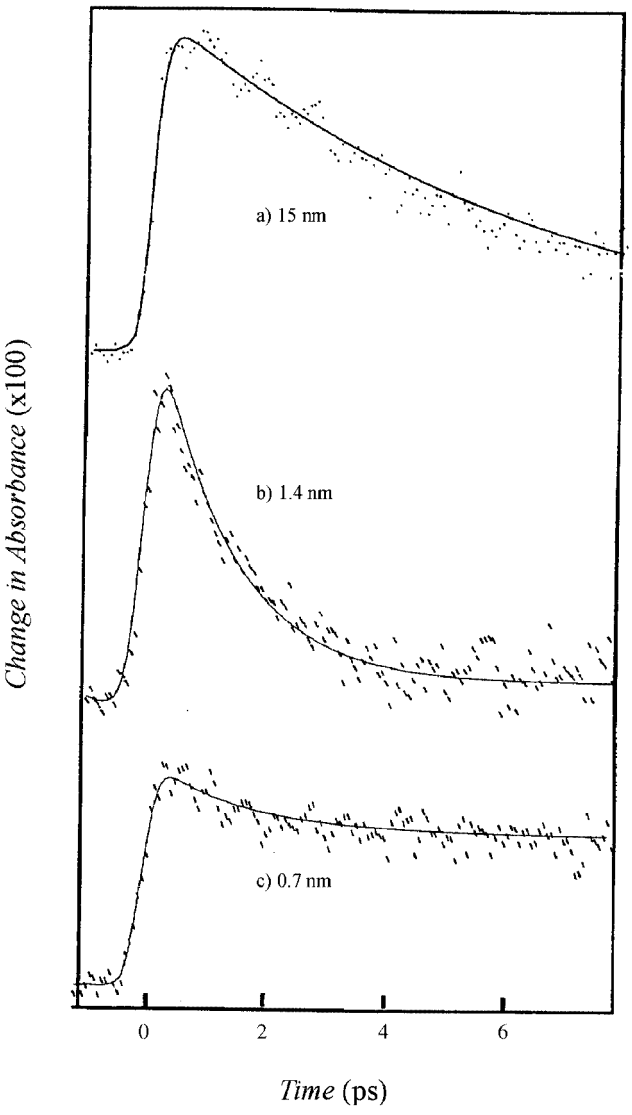

Figure 7. Relaxation behavior of gold nanoparticles of different sizes after excitation by femtosecond laser pulses

As we can see, the relaxation speed increases from the 15 nm particles to Au_{55}, also compared to the bulk. This effect is explained by the weakening of the electron-plasmon interaction, and the increase of the electronic collision-rate on the surface. For Au_{13} it decreases due to the existence of localized electrons. This cluster behaves like a molecule, whereas Au_{55} represents the very last "metal" before the typical molecular region begins. This example demonstrates that the decision "metal or not", cannot be precisely answered. As shown, optically Au_{55} is definitely no longer a colloid, and we have just learnt that it is not yet a molecule!

Probably the most informative method for studying the electronic situation inside a nanoparticle is to measure its current-voltage characteristics under different conditions. This can be performed by bringing an individual particle, bearing a non-conducting protecting shell (usually the li-

gands), into contact with two electrodes to which a variable voltage is applied. The insulating barrier is necessary to make tunnelling of individual electrons observable, as is indicated in Figure 8.

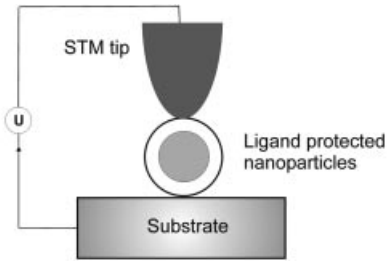

Figure 8. Sketch of a tunnelling contact consisting of an STM tip, a ligand-protected metal nanoparticle and a conducting substrate

The barrier conditions are responsible for the electron transport. Among others, they depend on the temperature. Owing to the relationship $E_C = e^2/2C >> k_BT$ (E_C = electrostatic energy, C = capacity of the island between the electrodes, k_BT = thermal energy), the thermal energy should be small in order to observe Single Electron Tunnelling (SET). If not, uncontrolled electron transitions occur. This fact was demonstrated by placing a ligand-protected 17 nm Pd particle next to two platinum tips.[66] At 295 K the particle exhibits a linear current-voltage ($I-V$) relationship and therefore indicates metallic behavior (Ohm Law). However, when measured at 4.2 K, a so-called Coulomb gap is observed: if k_BT is small enough, tunnelling of a single electron onto the particle blocks the transfer of a second one, due to Coulomb repulsion, until an appropriate voltage is reached.

$Au_{55}(PPh_3)_{12}Cl_6$ clusters on gold substrates have been investigated by bringing individual particles into contact with an STM tip so that information on $I-V$ characteristics can be gained. The result is very exciting: these particles indeed show well-expressed Coulomb blockades already at room temperature, as we can see in Figure 9.[67]

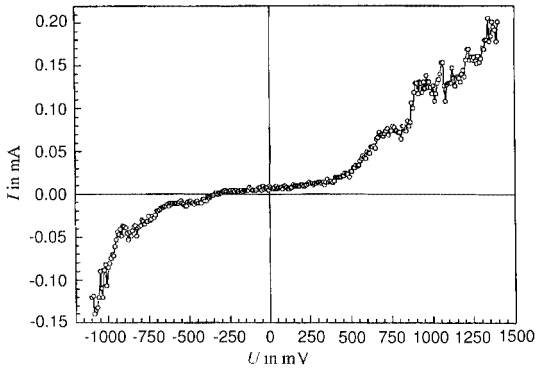

Figure 9. Room temperature $I-V$ characteristics of an individual $Au_{55}(PPh_3)_{12}Cl_6$ cluster indicating a well-expressed Coulomb blockade

This means that these 1.4 nm, ligand-protected particles behave as single electron-switches at room temperature! This opens up unexpected future applications in nanoelectronics.

The same Au_{55} species have very recently been studied by the same technique, however at 7 K under ultra high vacuum (UHV) conditions.[68] This method allows one to acquire not only tunnelling spectra, but also detailed images of individual particles. Figure 10 shows one of them together with a space-filling model in the corresponding orientation.

The light dots in Figure 11 indicate the positions of the phenyl rings of the PPh_3 ligands and **a** and **b** show two different sites where the STM tip was positioned for recording the tunnelling spectra: **a** above a C_6H_5 ring, **b** on the side of the ring, but with the same distance from the gold surface. Figure 11**A** shows the Coulomb blockade, which is the same size for both positions, indicating that the ligands do not visibly contribute to the tunnelling process;

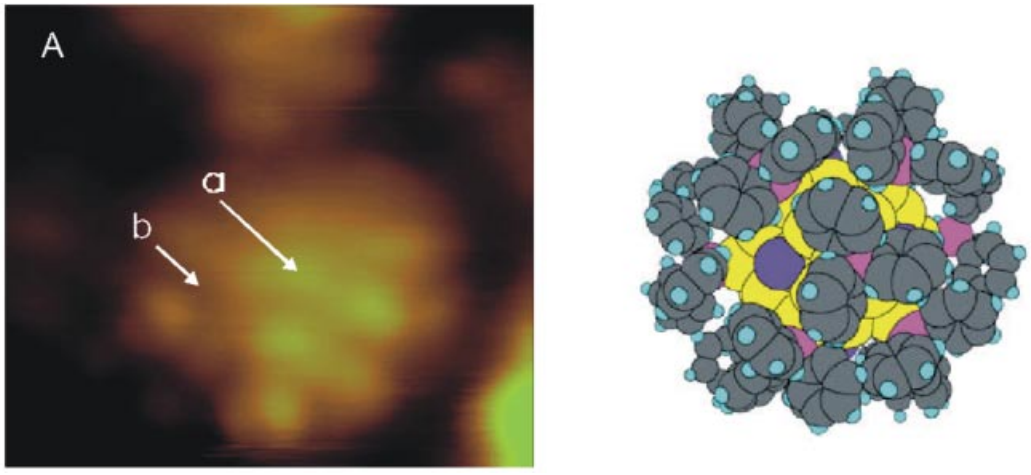

Figure 10. STM image of an individual $Au_{55}(PPh_3)_{12}Cl_6$ cluster at 7 K under UHV conditions together with a full-space model; the light dots indicate phenyl rings; the positions **a** and **b** indicate where the measurements have been performed to yield the $I-V$ characteristics in Figure 11

they simply act as distance holders. Still more interesting is the high resolution of the blockade region by using d*I*/d*V* instead of *I* (**B**). The arrows indicate conductivity signals which coincide precisely for both positions. For the very first time the existence of discrete energy levels inside the Au_{55} core could be proven. The occupied as well as the unoccupied levels are visible, due to conductivity oscillations. The average level spacing in vicinity to the Fermi level is about 170 meV.

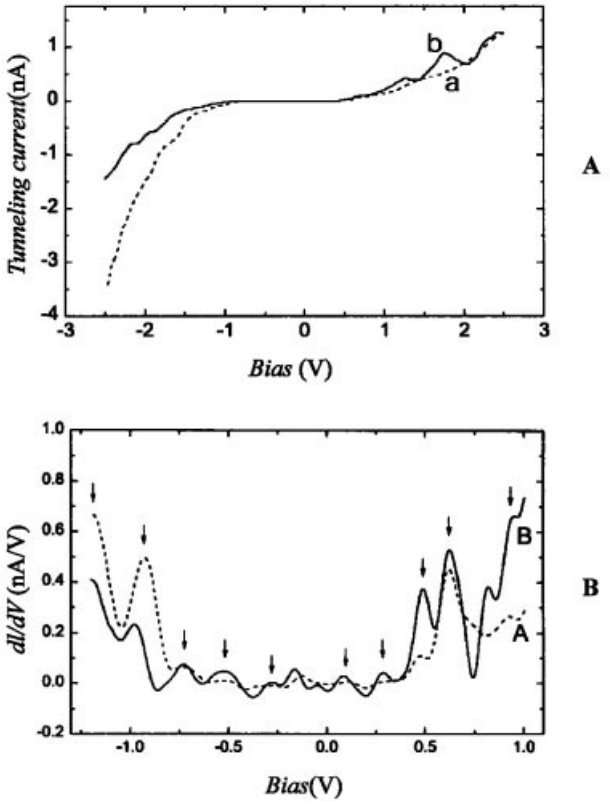

Figure 11. A) $I-V$ characteristic of an individual $Au_{55}(PPh_3)_{12}Cl_6$ cluster at 7 K under UHV conditions; **a** and **b** indicate equivalent Coulomb blockades although measured at different positions on the cluster's surface; B) d*I*/d*V* characteristic of the same particle indicating discrete electronic energy levels (arrows) in the Au_{55} cluster core

This experiment now justifies the expression "artificial atom" for those quantum dots and proves the assumptions of paragraph 4.1 that on the way from bulk to molecule at some point a situation arises where the electronic band structure begins to form discrete energy levels.

As a consequence of these unique properties it seems interesting to study the electron-transfer processes between the quantum dots. This was done for three-dimensionally organized Au_{55} clusters with variable distances.[69] However, as it turned out, it is not only the distance between the nanoclusters which determines the activation energy for the charge transfer, but also the nature of the interlinking species and the kind of linkage. If the clusters are simply separated from each other by ligand shells of different thickness or by non-covalently binding spacer molecules (ionic interactions), there is indeed only a simple linear relation between cluster-cluster distance and activation energy to be observed. On the contrary, if spacer molecules linking the particles via covalent S−Au bonds are used, it is not the distance that contributes decisively to the activation energy, but the chemical nature of the spacers. Figure 12 illustrates these results.

5. Approaches to Two-Dimensional Organizations

The two- and in some respect also the one-dimensional organization of metal nanoparticles is very relevant since one can think about the use of these particles in nanoelectronics only in an organized form. This is why numerous groups worldwide are dealing with this problem. It is again gold that plays an important role because of the easy availability of gold nanoparticles and their resistivity to air. So, there is a vast amount of reports, mainly on regular 2D arrangements of gold nanoparticles, most of them in the size regime of a few, up to 15 and 20 nm. Here we will only focus on recent results of organized Au_{55} clusters, since they are of promising electronic nature, as has been discussed in section 4.

After numerous attempts, rather extended self-assembled monolayers of $Au_{55}(Ph_2PC_6H_4SO_3H)_{12}Cl_6$ and of $Au_{55}(PPh_3)_{12}Cl_6$ became available.[70−72] The acidified cluster gives hexagonal and square structured 2D arrangements on poly(ethyleneimine) (PEI) films, whereas the neutral species is best organized at the phase transition between water and dichloromethane, supported by a layer of poly(vinylpyrrolidone) (PVP) or, still better, of poly(*p*-phenylene ethynylenes) (PPE). Although there is no doubt that PEI acts as a basic surface towards the SO_3H-modified Au_{55} cluster, the role of PVP and PPE in connection with $Au_{55}(PPh_3)_{12}Cl_6$ is somewhat more delicate. Relatively strong interactions, like those between the acidified cluster and PEI, prevent formation of extended ordered layers due to the lack of flexibility of the particles. On the contrary, PVP and PPE interact only weakly with the PPh_3-covered cluster, probably via hydrophobic-hydrophobic and π-π interactions, respectively. These weak forces between the clusters and the supports enable the formation of perfect arrangements since the particles are only weakly attracted and are allowed to find the best order. Figure 13 shows TEM images of cut-outs of square planar (**a**) and hexagonal (**b**) arrangements of Au_{55} clusters, generated on PEI and PPE, respectively.

An interesting electrical behavior of these ordered monolayers was observed when conductivity measurements were carried out.[73] Monolayers deposited between two tungsten electrodes on silica surfaces, 50−150 nm apart and 25 nm in height, and prepared on PVP films, as described above, were checked by scanning electron microscopy (SEM). Due to charging effects of the electron beam (10 keV, 10 s) the layers become conductive in the pA region in contrast to a not measurable conductivity without irradiation. However, if irradiation occurs on only one of the electrodes and part

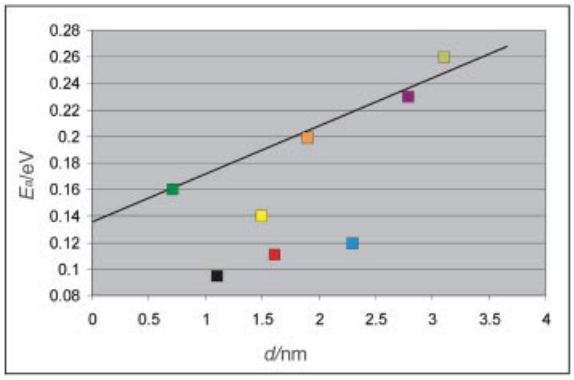

Covalently Linked **Linking System**	Distance nm	E_a (eV)
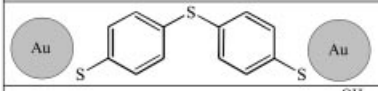	1.1	0.095
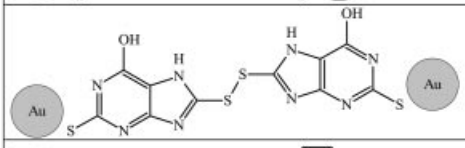	1.6	0.11
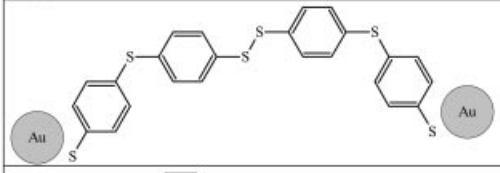	2.3	0.12
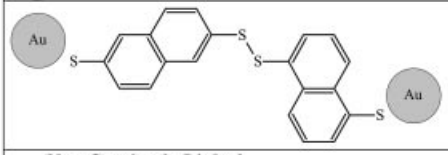	1.5	0.14
Non-Covalently Linked **Linking System**	Distance nm	E_a (eV)
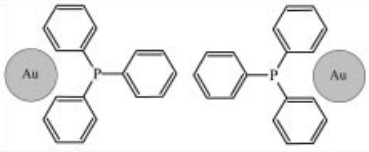	0.7	0.16
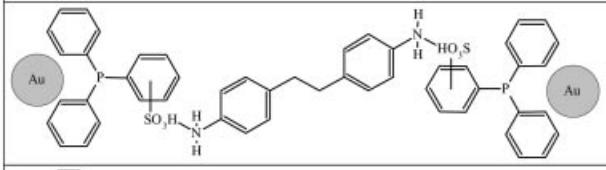	1.9	0.20
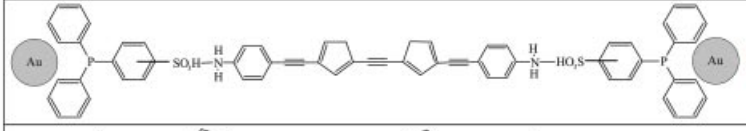	2.8	0.23
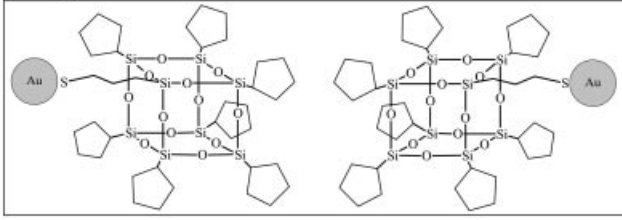	3.1	0.26

Figure 12. Activation energies for Au_{55} clusters of varying distances, covalently and non-covalently linked

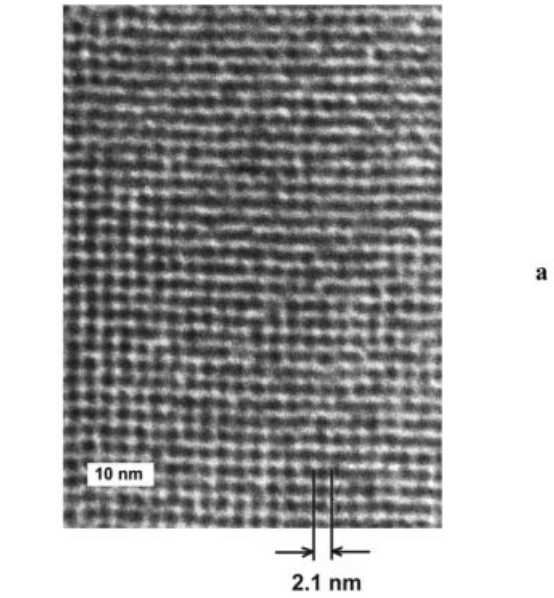

Figure 13. TEM images of square planar (**a**) and hexagonal (**b**) monolayers of ligand-stabilized Au_{55} clusters

of the monolayer, diode-like behavior is observed. The $I-V$ characteristics depend on the contact distances, the irradiation time, the energy of the electron beam, the exposure time and finally on the irradiated area. Figure 14 shows a typical diode curve (**a**) gained with a set-up of electrodes of 122 nm distance (**b**) and an exposure time of 5 s at 16 keV.

In all cases the systems relax in the course of 24−36 h after switching off the voltage. However, reactivation is possible, indicating that there is no chemical change with respect to the starting situation. In order to explain this unusual behavior we assume that electrons from irradiation, trapped in the silica layer, create so-called image charges in the cluster layer. This activation makes the particles order themselves so as to reach a minimum energy arrangement with a maximum delocalization of the additional electrons. The rearrangement of the clusters may happen very quickly due to the electron irradiation, whereas the deactivation takes much more time.

Self-organization of quantum dots must be considered only as a first step for collecting information on their electronic interchange. However, for practical use with respect to future data storage or related applications, it is necessary to create artificial architectures. A first approach as to how this high goal might be reached will be described below. It is based on the generation of appropriately modified surfaces.[74] A metallized AFM tip was used as a tool for transforming methyl groups of a self-assembled monolayer into carboxylic functions by electrical pulses under air. The total process is sketched in Figure 15.

The COOH groups are used to add silane molecules to C=C double bonds which can then be transformed to thiol-functionalized derivatives. Finally, water-soluble $Au_{55}(Ph_2PC_6H_4SO_3Na)_{12}Cl_6$ clusters are chemisorbed from solution by the thiol functions. The width of the traces simply depends on the quality of the tip. As we can see from Figure 16, arranged dots of clusters (a), as well as single gold clusters between wires made of single rows of particles (b), have been created, and of course any other structure could be created.

There is no doubt that these structures offer great advantages compared with self-assembled arrangements. How-

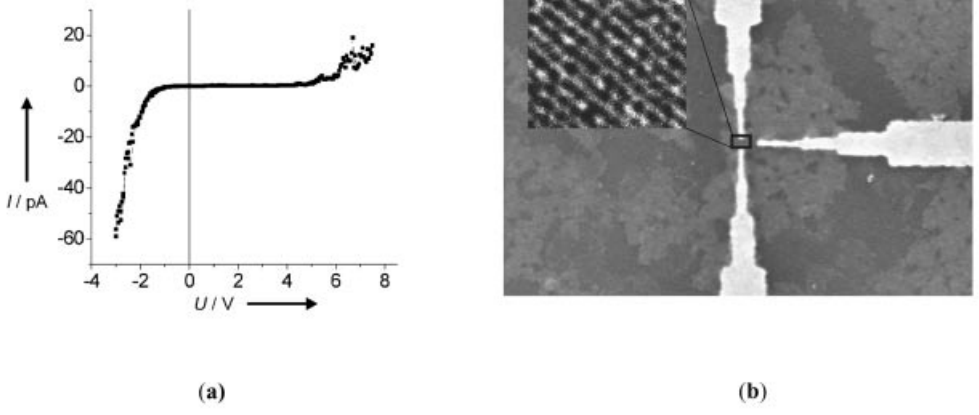

Figure 14. Diode behavior of $Au_{55}(PPh_3)_{12}Cl_6$ monolayers, in contact with tungsten electrodes on SiO_2, after partial irradiation with an electron beam

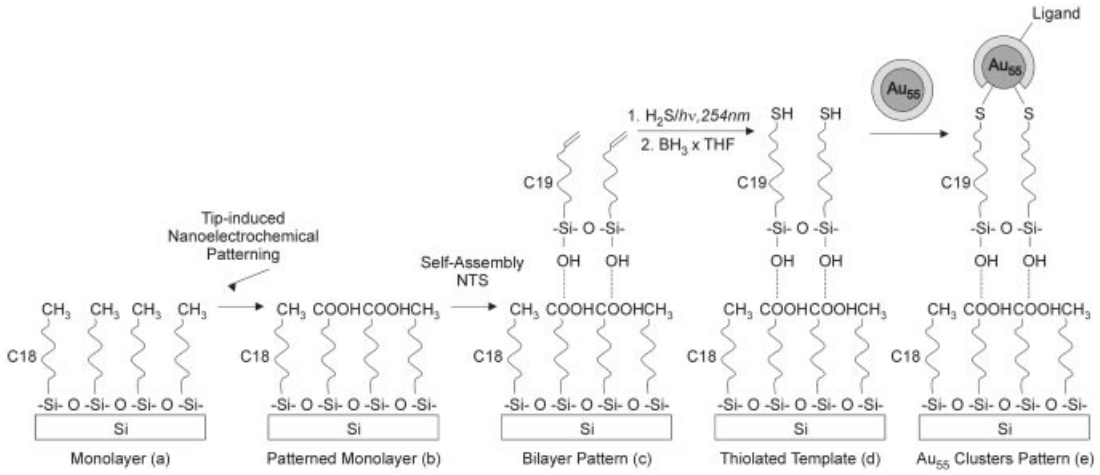

Figure 15. Sketch of the generation of SH-functionalized patterns on a Si wafer to trap Au_{55} clusters

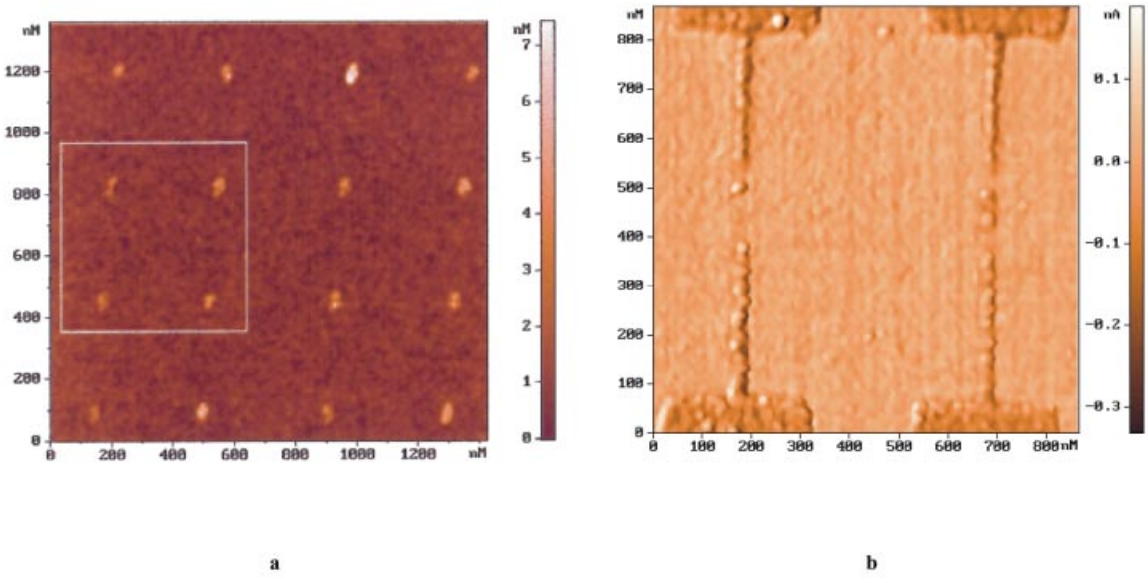

Figure 16. a, b Patterns of Au_{55} clusters deposited on chemically modified surfaces as shown in Figure 15

ever, it is also clear that there is still a lot of work to be done to develop a working system. One major problem will be to study individual quantum dots and to connect them with the outer world. There are ideas on how to do this, but many efforts will be necessary to reach this goal.

6. Chemical Activity

Two main aspects concerning chemical activity of gold nanoparticles will be treated in this chapter: ligand-exchange reactions and catalytic activity. Ligand-exchange reactions are quite common and are used to change solubility or to introduce special functions. Catalytic properties of gold nanoparticles are currently developing into an attractive and important field in gold chemistry. Therefore, a rather detailed discussion of catalytic properties will be found in this section.

6.1 Ligand-Exchange Reactions

As discussed in chapter 2.2, wet chemical syntheses of gold nanoparticles are always linked to the presence of protecting ions or molecules since without them, coalescence would quickly occur. As an example we should remember the famous citrate route for the generation of 15−20 nm gold colloids. Without any other stabilizing species the gold particles are covered by excessive citrate, but also by Cl^- ions and acetone dicarboxylate, an oxidation product of citrate. These species bind strongly enough to keep the colloids in solution for a long time. However, they can easily be substituted by stronger binding molecules. For instance, the water-soluble phosphane $P(C_6H_4SO_3Na)_3$ can easily re-

move the original ions and molecules to form such a strong ligand-shell that these gold nanoparticles can even be isolated as solid products.[27] We must assume that phosphane molecules on the surfaces of gold nanoparticles are rather mobile in solution. This was shown long ago by ^{31}P NMR investigations of $Au_{55}(PPh_3)_{12}Cl_6$ with excess PPh_3.[75] Gradual addition of free PPh_3 to cluster solutions causes a shift of the ^{31}P signal from $\delta = 34$ ppm towards that of free phosphane ($\delta = -5.5$ ppm). This is due to the fast exchange processes between free and coordinated PPh_3 molecules. The mobility of ligand molecules is also the reason why $Au_{55}(PPh_3)_{12}Cl_6$ is rather labile in solution (due to the loss of PPh_3), and as a consequence, coalescence processes are inhibited. The formation of the water-soluble compound $Au_{55}(Ph_2PC_6H_4SO_3Na)_{12}Cl_6$, from $Au_{55}(PPh_3)_{12}Cl_6$, dissolved in dichloromethane, is also based on that ligand mobility. The fact that the water-soluble derivative is formed in quantitative amounts is due to the phase transfer from CH_2Cl_2 to H_2O and to the somewhat better coordination of $Ph_2PC_6H_4SO_3Na$ compared to PPh_3.

The high mobility of phosphanes on gold-particle surfaces can be used to substitute them with stronger ligands, above all by thiols. As already mentioned in section 2.2, the thiol-functionalized silsesquioxane $(cyclopentyl)_7Si_8O_{12}(CH_2)_3SH$, as well as the anionic thiol $[B_{12}H_{11}SH]^{2-}$, quantitatively substitute phosphanes in Au_{55} clusters with the help of phase transitions.[35,34] The alkyl-terminating silsesquioxane, readily soluble in apolar solvents such as pentane or hexane, transfers the water-soluble cluster $Au_{55}(Ph_2PC_6H_4SO_3Na)_{12}Cl_6$ into the pentane-soluble derivative with silsesquioxane ligands, whereas the dichloromethane-soluble $Au_{55}(PPh_3)_{12}Cl_6$ becomes water-soluble if reacted with $Na_2[B_{12}H_{11}SH]$. Figure 17 illustrates these transfer reactions that indicate that the same cluster particle can change its solubility from dichloromethane to pentane or even to water.

A very special kind of "phosphane substitution" in $Au_{55}(PPh_3)_{12}Cl_6$ is observed when the latter is reacted with an excess of a fourth-generation dendrimer bearing 96 terminal SH functions.[76] The excess dendrimer obviously re-

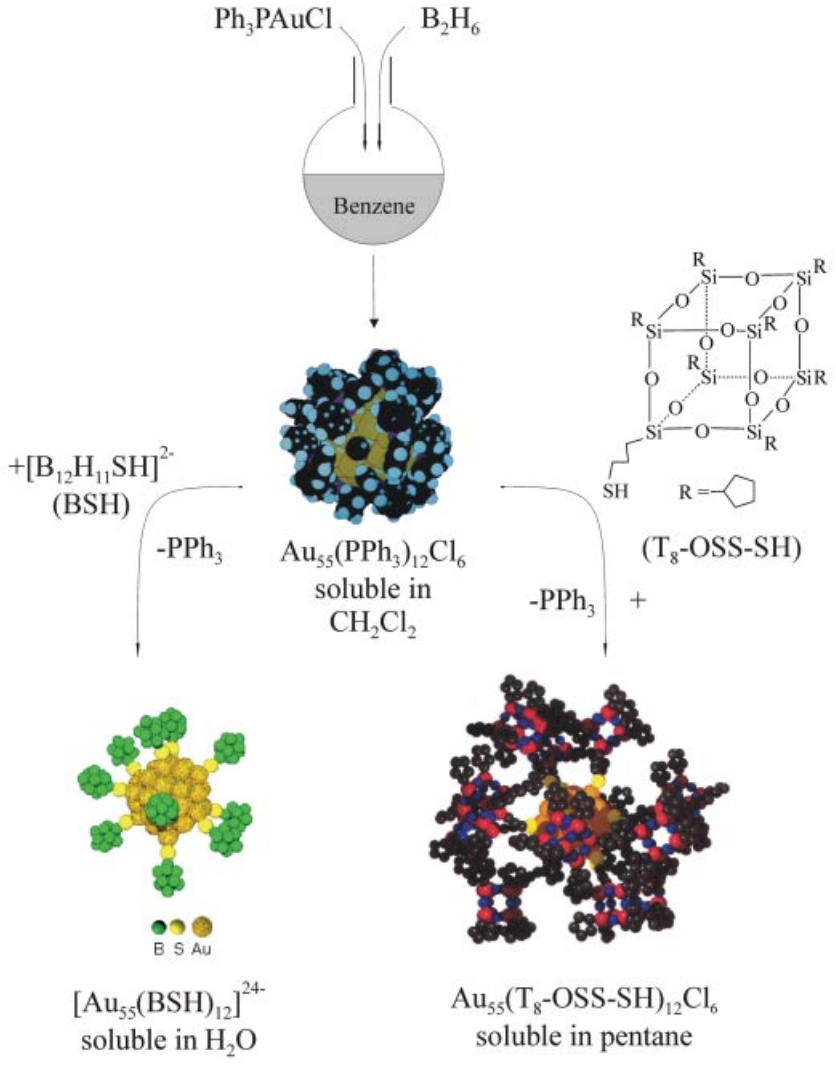

Figure 17. Sketch of synthetic routes to $Au_{55}(PPh_3)_{12}Cl_6$ and some of its derivatives

moves all the phosphanes from the clusters' surface. However, Au−Au interactions between the bare clusters occur and the coordination of dendrimers is not observed . Consequently, naked Au_{55} particles grow to regular microcrystals inside a matrix of dendrimers.

Finally, a very unexpected behavior of naked Au_{55} clusters will be mentioned. While surfaces of bulk gold and particles of 7.9, 2.9, 1.6, 1.3, and <1 nm are all oxidized when deposited on top of a silicon wafer and exposed to atomic oxygen, bare Au_{55} resists these extreme oxidative conditions.[77] Moreover naked Au_{55} clusters are formed in oxygen plasma by burning off the ligand shell, as can clearly be followed from the X-ray photoelectron spectra. Only traces of oxides appear, as indicated by the presence of a weak shoulder, the main part of the particles remaining unchanged. Figure 18 shows the Au-4f photoelectron spectra of the oxidized particles including Au_{55} clusters.

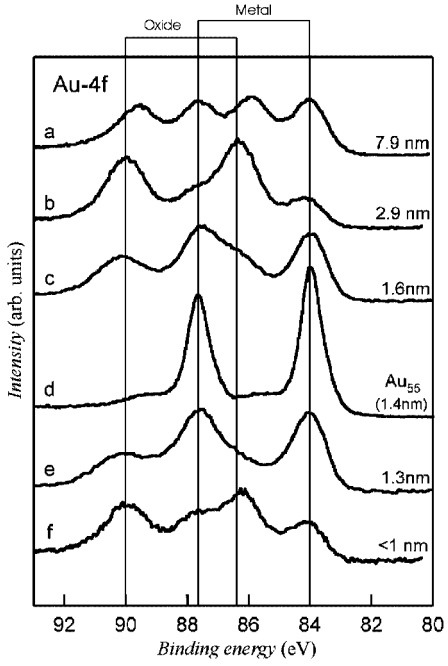

Figure 18. X-ray photoelectron spectra of various gold particles after exposure to an oxygen plasma; all particles except for Au_{55} show well expressed gold oxide signals

In all cases except for Au_{55} there are well-developed signals for gold oxides. This phenomenon has led to the formulation that Au_{55} is "nobler than bulk gold".[78] As an explanation of this unique behavior it is assumed that it is the special stability of Au_{55} as a closed-double-shell structure. It is excluded that a special electronic situation might cause this inertness. As a consequence it can be predicted that other full-shell clusters such as Au_{147} or Au_{309} etc. should also resist oxidation. Owing to the non-availability of these particles, this prediction cannot yet be proven . However, it can be suggested that these gold full-shell clusters might act as special oxidation catalysts.

6.2 Nanoparticulated Gold in Modern Catalysis

6.2.1 Historical Survey

In contrast to the catalytic potential of its neighbors silver and platinum,[79] bulk gold metal appeared for long time an essentially useless material for catalysis.[80,81]

The first documented exhibition of catalytic activity of bulk gold occurred at the beginning of the past century when Bone and Wheeler showed in 1906 that gold foils catalyse the combustion of dihydrogen and dioxygen to give water.[82] The relevant paper is remarkable in that the authors also collected good quantitative kinetic data on the same reaction. It was believed for a long time that the inability of Au^0 to activate (chemisorb) O_2 in any catalytic oxidation reaction was a straight manifestation of its thermodynamic reluctance to form metal oxides (ΔH_f^0 of Au_2O_3 = +19.3 kcal·mol^{-1} [81]). Ironically, the extremely facile Au^0-catalyzed oxidation of CO to CO_2 by O_2 is the most striking result in Au^0-catalytic chemistry, but only when Au^0 occurs as metal nanoparticles supported on suitable metal oxides.

Information on the catalytic chemistry of Au^0, obtained in the decades following Bone and Wheeler's observation, was not considered very exciting.[83] However, in the course of the seventies, three major observations were made: a) Au^0 supported on silica (0.01−0.05%) was found by Bond and Sermon to catalyse the hydrogenation of alkenes at 373 K, with no effect on the potentially concomitant double bond migration reaction,[84] b) Au^0 supported on MgO or Al_2O_3 was found by Galvagno and Parravano to catalyse oxygen- and hydrogen-transfer reactions [85] and c) a green $Au(O_2)$ molecular species with side-on bonded dioxygen could be obtained at extremely low temperatures in a solid matrix.[86,87] Most interestingly, this very remarkable molecule was found to react with CO at a suitable temperature to give eventually free Au^0 and CO_2. Indeed this was a prophetic observation!

Among the many good review papers quoted in this report, the 2002 review by Choudhary and Goodman as a general and critical reading on Au^0 catalytic chemistry is particularly recommended.[88]

6.2.2 Synthesis of Supported Gold(0) Catalysts

The overall grey scenario of Au^0 catalytic chemistry became suddenly lightened in 1989 when Haruta et al. reported on a real breakthrough in this field of research.[89] They observed, in fact, that the oxidation of CO to CO_2, a technologically relevant reaction under various circumstances, could be effectively catalyzed by supported-Au^0. Moreover, it was later observed that the reaction occurs even at 200 K.[90] It soon became apparent that the key to this success was twofold: a) the presence of gold nanoparticles in the gold catalysts and b) a strong co-catalytic role played by the support that had to be an inorganic oxide such as Fe_2O_3, TiO_2, or Co_3O_4. It also became apparent that the optimal nanocluster diameter was ca. 3 nm, the size at which metal nanoclusters start to exhibit quantum-size behavior.[91,92]

This discovery promoted an incredible amount of research and an avalanche of papers and patents in a manifestation of a modern-day "gold rush".

We believe that the catalysis community was particularly stricken by Haruta's discovery in that it represented an unprecedented example of both extreme catalyst structure-sensitivity and of an impressive co-catalytic role played by the metal-supporting microphase (vide infra). In fact, the issue of catalyst preparation and the full understanding of the role of the support appeared immediately very complex, still to be fully evaluated nowadays and, in this connection, the reader is referred to an authoritative review paper by Bond and Thomson who critically examined the matter in the year 2000, in terms of both consensual and disputed literature observations and to other general as well as specific readings.[93−99]

Supported gold nanoparticles (1−5 nm) are currently prepared according to a dozen or so rather different methods, which can be reduced in essence to three major procedures.

The precursor of Au^0 is mixed with the precursor(s) of the supports (or with the support itself) to give a system that, after controlled calcination, produces Au^0/S catalysts. The metal nanoparticle's size is controlled by the calcination temperature, and lower temperatures seem to favor the formation of smaller particles.[100,101]

The precursor of Au^0 is deposited or grafted onto the surface of the support, which has been pre-formed from the gas or from the liquid phase,[99] and subsequently thermally decomposed to give the Au^0/S catalysts. We would like to mention, in this respect a recent outcome from these laboratories, i.e. the preparation of an Au^0/resin catalyst obtained from the chemical reduction of an $Au^{I,III}$/resin-macromolecular complex prepared simply by complexation of aqueous $AuCl_3$ with a thioethereal gel-type resin.[102]

The Au^0 nanoparticles are pre-produced in a given solution where they are stabilized by soluble polymers[103] or by kinetic conditions, and subsequently left to be adsorbed by the surface of the desired support particles.[104]

As anticipated above, it is now widely accepted that at least for CO oxidation and for the water gas shift reaction, catalytic activity depends critically on the metal nanoparticles' size, on the nature of the support and on the detailed synthetic procedure. In this context, the deposition precipitation (DP) procedure is generally widely considered the most suitable one (Scheme 1).

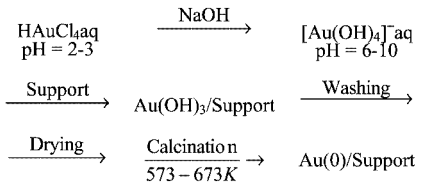

Scheme 1. Deposition precipitation procedure to give Au/S catalysts[99]

In fact, DP turns out to be particularly suitable for producing hemispherical (ca. 3 nm) nanoparticles (Figure 19) that are believed to cause a particularly strong attractive force between a given nanoparticle and the crystal lattice of the support located just underneath it.

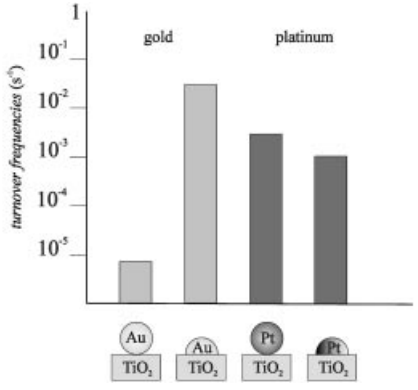

Figure 19. Dramatic effect of the Au^0-support interaction on the CO oxidation reaction rate over spherical vs. hemispherical nanoclusters; it is important to note the quite different effect of the nanoclusters's shape on the action of Pt^0

This phenomenon has two major consequences: i) a marked thermal stability of the Au^0 nanoparticles (thus contrasting the particles' coalescence) and ii) a peculiar local electronic situation at the lattice interface of the metal nanoparticles and the support, that is likely to be responsible for the particular mechanism of oxygen transfer to chemisorbed carbon monoxide to give carbon dioxide (see below).

6.2.3 Nanoparticulated-Gold(0) on Metal Oxides: Facile Oxidation of Carbon Monoxide to Carbon Dioxide

No measurable oxidation of CO by O_2 on micro-sized (in fact "bulk") supported-Au^0 is observed at ambient conditions. On the contrary, if a mixture of CO and O_2 is allowed to interact with 2−5 nm gold particles dispersed on the same support, under identical Au^0 molar fraction, a rapid and quantitative oxidation to CO_2 is observed even at 200 K.[90]

Wallace and Whetten observed an effective formation of CO_2 when CO and O_2 were reacted with Au_6^- in the gas phase (Figure 20).[105] Moreover, theoretical calculations carried out by Lopez and Norskov[106] revealed that isolated Au_{10} clusters are expected to catalyse CO oxidation even below room temperature. All these observations seem to provide an explanation of the established activity of the nanoparticles' surface gold atoms in the CO oxidation. However, reality is more complex than that!

An Au^0 nanoparticle of 2−3 nm in size, exposes ca. 50% of its atom constituents to the action of gaseous species that find possible reaction sites at the edge-, corner- or step-sites of the nanoparticle surface. Consequently, we might consider that the electronic and geometrical features of these potential activation sites are related to Au_6^- and to

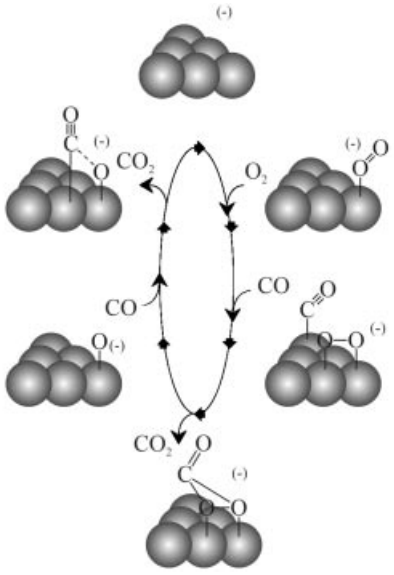

Figure 20. Schematic illustration of the formation of CO_2, catalyzed by Au_6^- in the gas phase

Au_{10} molecular clusters. However, this is probably not the case and several authors[93,88,99] provide evidence that, while CO is activated by its end-on coordination to the nanocluster surface, O_2 is activated by a combined action of the Au^0 nanoparticle surface and of the nanoparticle-support interface surface (Scheme 2).

$$CO + Au(0)/TiO_2 \text{ ---> } Au(0)(CO)/TiO_2$$

$$O_2 + Au(0)/TiO_2 \text{ ---> } Au(0)/TiO_2 \cdots O_2$$

$$CO + Au(0)/TiO_2 \cdots O_2 + Au(0)(CO)/TiO_2 \text{ ---> } CO_2 + Au(II)(CO)(O)/TiO_2 \cdots Au(0)/TiO_2$$

$$Au(II)(CO)(O)/TiO_2 \text{ ---> } CO_2 + Au(0)/TiO_2$$

Scheme 2. Reaction steps proposed for CO oxidation to CO_2 by Au^0/TiO_2

Apparently, this synergic mechanism makes Au^0/S catalysts uniquely active in CO oxidation to such an extent that Au^0/S is able to catalyse CO oxidation even more rapidly than H_2 oxidation.[107] This observation is a fundamental

Table 1. A selection of reactions relevant to chemical processing, catalyzed by supported gold(0)

Entry	Reaction	Catalyst	Remarks	Ref.
1	CH_2=CH-CH=CH_2 + H_2 → butenes	Au/S	gas phase, structure and support insensitive	[109]
2	CH_2=CH-C(O)H + H_2 → allyl alcohol	Au/ZrO_2	gas phase, structure sensitive	[110]
3	R-OH $\xrightarrow{air}$ R-C(O)H	Au/SiO_2	gas phase	[111]
4	R-OH, MeCO, Ph-CH_3 $\xrightarrow{air}$ catalytic combustion	Au/Fe_2O_3	gas phase	[112]
5	*o*-hydroxybenzyl alcohol $\xrightarrow{O_2}$ salicylic aldehyde	Au/Fe_2O_3	liquid phase, 50 °C, 1 atm, chemoselective	[113]
6	ethane-1,2-diol $\xrightarrow{O_2}$ glycolate	Au/C	liquid phase (H_2O), 70 °C, 2 atm	[114]
7	diols $\xrightarrow{O_2}$ hydroxymonocarboxylates β-amino alcohols $\xrightarrow{O_2}$ β-amino acids aliphatic aldehydes $\xrightarrow{O_2}$ carboxylic acids D-glucose $\xrightarrow{O_2}$ gluconic acid	Au/C or Au/TiO_2	liquid phase (H_2O), 70–85 °C, 1–3 atm	[103]
8	citral $\xrightarrow{H_2}$ geraniol + nerol	Au/Fe_2O_3	liquid phase, ethanol, 1 atm, 60 °C, chemoselective (95%) hydrogenation of C=O, 100% conversion	[115]
9	benzalacetone $\xrightarrow{H_2}$ phenyl-3-buten-2-ol	Au/Fe_2O_3	liquid phase, ethanol, 1 atm, 60 °C, chemoselective (60%) hydrogenation of C=O, 100% conversion	[116]
10	$H_2 + O_2 \rightarrow H_2O_2$	Au·Pd/Al_2O_3	liquid phase, methanol, 2 °C, 97 atm, chemoselective (50%)	[117]
11	aromatic amines $\xrightarrow[MeOH]{CO,\ O_2}$ carbamates	Au/resin	solvent-free, P_{CO} = 40 atm, P_{O2} = 40 atm, 175 °C. Good conversion and selectivity	[118]
12	propylene + O_2 → propylene oxide	Au/Ti-MCM48	gas phase, presently limited yields	[114]

premise to the commercial development of fairly innovative dihydrogen-air PEM (Polymer Electrolyte Membrane) fuel cells for vehicle propulsion and auxiliary power units. In this context, CO-free dihydrogen has to be employed and various Au^0/S catalysts, in particular $Au^0/Al_2O_3/MgO/MnO$, are known to allow the removal of CO (ppm levels) from the dihydrogen stream that feeds the fuel cells at 60−100 °C (PROX reactor),[108] without a significant consumption of dihydrogen. The technical problem to be solved for a straight commercialization of PROX technology is the achievement of a suitable stability of the catalyst itself.

6.2.4 Gold(0)-Based Catalysis for Chemical Processing

Haruta's discovery, which was published in 1989, not only produced an explosion of interest for the catalytic chemistry of gold nanoparticles, mainly around the problem of CO and O_2 activation, but it also promoted a huge amount of research on a variety of possible applications of gold nanoparticles in pollution-control technologies and in chemical processing, i.e. in the potential industrial synthesis of commodities, semi-commodities, and fine and specialty chemicals.

A few recent examples of these valuable prospects are presented in Table 1.

It is apparent from Table 1 that the prospects for employing supported nano-sized-Au^0 in industrial catalysis are excellent, both in the gas and the liquid phase, with good prospects for using water as the solvent[103][114] in oxidation processes. The facile synthesis of H_2O_2 from O_2 and H_2 seems to be one of the major listed results that allow us to imagine the achievement of small-scale industrial facilities for the production of hydrogen peroxide.

6.2.5 Ongoing and Future Applications of Gold(0)-Based Catalysis

This topic is presented and discussed in references 93, 96, 99 and 119.

A peculiar current application is provided by Au^0 deposited on Fe_2O_3, supported on a zeolite wash-coated honeycomb. This sophisticated setup catalyses effectively the oxidative decomposition of bad smelling alkylamines (with a minimal production of N_2O) that are responsible for the unpleasant atmosphere in toilets ("odour eaters").[99]

Au^0/La_2O_3, integrated with Pd/SnO_2 and Ir/La_2O_3 is likely to become employed as a catalyst for the oxidative decomposition of dioxins coming from incinerator outlet gases at temperatures below 473 K.[99]

The long-awaited direct epoxidation of propylene is expected to become an Au^0-catalyzed synthetic technology once the yield in propylene oxide has been improved to ca. 10% and this goal seems to be feasible on Au^0/Ti-MCM48.[99]

Composite films of Co_2O_3 nanocrystals (5−10 nm) are expected to form the basis for optical sensors able to simultaneously detect H_2 and CO at 1% levels.[93]

Au^0/S catalysts are likely to become key components of CO safety masks and of devices for the efficient removal of CO from contaminated atmospheres.[96,119]

Finally, a little-explored and quite promising sector of gold catalytic chemistry is the employment of Au^0/S catalysts in liquid-phase synthetic processes. The brilliant results obtained by a few research groups, even in water, (Table 1) are indeed promising, quite in line with the emerging view of "Green Chemistry".

"Although we are well past the beginning of the discovery of gold's catalytic potential, the best may be yet to come, and a golden future lies ahead" (G. C. Bond, 2002).[81]

Conclusions

Nanoparticulated gold has turned out to play an important role in various fields of nanoscience. Besides their unique color, gold nanoparticles became of scientific and technological interest because of their stability to air which means that they can be used even in nanosized form for many applications. Well-expressed quantum-size effects have been observed for particles smaller than 2 nm even at room temperature, making these artificial atoms valuable candidates for future nanoelectronics once appropriate techniques allow the generation of artificial structures on surfaces. The first steps in this direction look very promising. The moderate chemical reactivity of gold atoms on particle surfaces allows them to act as catalysts for distinct reactions, for example oxidation reactions. Indeed, there are several catalytic reactions where gold nanoparticles act as highly efficient catalysts.

It can be assumed that the use of particulated gold will dramatically increase in the near future in very different fields. Gold quantum dots may act as single-electron switches and transistors, at the latest when silicon technology has reached its physical limits. Gold nanowires as conducting contacts in nanoelectronics will also contribute to the progress of nanotechnology. A renaissance in gold catalysis seems to have started. Gold nanoparticles in combination with biomolecules are already at a point where even commercial applications in medical diagnostics have become known.

Another developing field is sensorics where gold nanoparticles might play the most important role. Other applications, not yet to be foreseen, may come up and make the next decades a "golden age".

Acknowledgments

The Alexander von Humboldt Foundation is gratefully acknowledged for a Scholarship provided to one of us (B. C.) in 2002.

[1] M. T. Franklin, K. J. Klabunde, in *High Energy Process in Organometallic Chemistry* (Ed.: K. S. Suslik), *Am. Chem. Soc.,* Washington D. C., **1987**, pp 246−259.
[2] M. Faraday, *Phil. Trans. Roy. Soc.* **1857**, *147*, 145.

[3] W. Ostwald, *Colloid-Zeitschrift* **1907**, *1*, 291.
[4] T. Castro, R. Reifenberger, E. Choi, R. P. Andres, *Phys. Rev. B* **1990**, *13*, 8548.
[5] G. L. Hornyak, M. Kröll, R. Pugin, Th. Sawitowski, G. Schmid, J.-O. Bovin, G. Karsson, H. Hofmeister, S. Hopfe, *Chem. Eur. J.* **1997**, *3*, 1951.
[6] *Optical Properties of Metal Clusters* (Eds.: U. Kreibig, M. Vollmer), Springer Series in Materials Science 25, Springer 1995.
[7] G. Mie, *Annal. Phys.* **1908**, *5*, 377.
[8] *Metal Vapour Synthesis* (Eds.: J. R. Blackborow, D. Young), Springer Verlag, New York 1979.
[9] J. S. Bradley, in *Clusters and Colloids. From Theory to Applications* (Ed.: G. Schmid), VCH, Weinheim 1994.
[10] A. Fojtik, A. Henglein, *Ber. Bunsen-Ges. Phys. Chem.* **1993**, *97*, 252.
[11] M. S. Sibbald, G. Chumanov, T. M. Cotton, *J. Phys. Chem.* **1996**, *100*, 4672.
[12] M. S. Yeh, Y. S. Yang, Y. P. Lee, H. F. Lee, Y. H. Yeh, C. S. Yeh, *J. Phys. Chem. B* **1999**, *103*, 6851.
[13] F. Mafuné, J. Kohno, Y. Takeda, H. J. Sawabe, *J. Phys. Chem. B* **2000**, *104*, 8333.
[14] F. Mafuné, J. Kohno, Y. Takeda, T. Kondow, H. J. Sawabe, *J. Phys. Chem. B* **2000**, *104*, 9111.
[15] H. Eckstein, U. Kreibig, *Z. Phys. D* **1993**, *26*, 239.
[16] Y. Niidome, A. Hori, T. Sato, S. Yamada, *Chem. Lett.* **2000**, 310.
[17] P. V. Kamat, M. Flumiani, G. W. Hartland, *J. Phys. Chem. B* **1998**, *102*, 3123.
[18] H. Kurita, A. Takami, S. Koda, *Appl. Phys. Lett.* **1998**, *72*, 789.
[19] A. Takami, H. Kurita, S. Koda, *J. Phys. Chem. B* **1999**, *103*, 1226.
[20] F. Mafuné, J. Kohno, Y. Takeda, T. Kondow, *J. Phys. Chem. B* **2001**, *105*, 9050.
[21] F. Mafuné, J. Kohno, Y. Takeda, T. Kondow, *J. Phys. Chem. B* **2002**, *106*, 7575.
[22] S. Stoeva, K. J. Klabunde, Ch. M. Sorensen, I. Dragieva, *J. Am. Chem. Soc.* **2002**, *124*, 2305.
[23] K. J. Klabunde, P. L. Timms, P. S. Skell, S. Ittel, *Inorg. Synth.* **1979**, *19*, 59.
[24] J. Turkevitch, P. C. Stevenson, J. Hillier, *Discuss. Faraday Soc.* **1951**, *11*, 55.
[25] A. Henglein, M. Giersig, *J. Phys. Chem. B* **1999**, *103*, 9533.
[26] S. Link, Z. L. Wang, M. A. El-Sayed, *J. Phys. Chem. B* **1999**, *103*, 3529.
[27] G. Schmid, A. Lehnert, *Angew. Chem. Int. Ed. Engl.* **1989**, *28*, 780.
[28] *Clusters and Colloids. From Theory to Applications* (Ed.: G. Schmid), VCH, Weinheim 1994.
[29] G. Schmid, R. Boese, R. Pfeil, F. Bandermann, S. Meyer, G. H. M. Calis, J. W. A. van der Velden, *Chem. Ber.* **1981**, *114*, 3634.
[30] G. Schmid, *Inorg. Synth.* **1990**, *7*, 214.
[31] G. Schmid, N. Klein, L. Korste, U. Kreibig, D. Schönauer, *Polyhedron* **1988**, *7*, 605.
[32] L. O. Brown, J. E. Hutchison, *J. Am. Soc., Chem.* **1997**, *119*, 12384.
[33] M. G. Warner, S. M. Reed, J. E. Hutchison, *Chem. Mater.* **2000**, *12*, 3316.
[34] G. Schmid, R. Pugin, W. Meyer-Zaika, U. Simon, *Eur. J. Inorg. Chem.* **1999**, 2051.
[35] G. Schmid, R. Pugin, J.-O. Malm, J.-O. Bovin, *Eur. J. Inorg. Chem.* **1998**, 813.
[36] M. Brust, A. Walker, D. Bethell, D. J. Schiffrin, R. Whyman, *J. Chem. Soc., Chem. Commun.* **1994**, 801.
[37] M. J. Hostetler, J. E. Wingate, C. J. Zhong, J. E. Harris, R. W. Vachet, M. R. Clark, J. D. Londono, S. J. Green, J. J. Stokes, G. D. Wignale, G. L. Glish, M. D. Porter, N. D. Evans, R. W. Murray, *Langmuir* **1998**, *14*, 17.
[38] N. R. Jana, L. Gearheart, C. J. Murphy, *Langmuir* **2001**, *17*, 6782.
[39] S. Chen, K. Kimura, *Langmuir* **1999**, *15*, 1075.
[40] K. Akamatsu, J. Hasegawa, H. Nawafune, H. Katayama, F. Ozawa, *J. Mater. Chem.* **2002**, *12*, 2862.
[41] J. P. Spatz, S. Mößmer, M. Möller, *Chem. Eur. J.* **1996**, *12*, 1552.
[42] J. P. Spatz, A. Roescher, M. Möller, *Adv. Mater.* **1996**, *8*, 337.
[43] M. Möller, J. P. Spatz, A. Roescher, S. Mößmer, S. T. Selvan, H.-A. Klok, *Macromol. Symp.* **1997**, *117*, 207.
[44] J. P. Spatz, A. Roescher, M. Möller, *Polymer Preprints, Am. Chem. Soc.* **1996**, *36*, 409.
[45] M. Möller, J. P. Spatz, *Curr. Opin. Colloid Interface Sci.* **1997**, *2*, 177.
[46] J. W. Slot, H. J. Geuze, *Eur. J. Cell Biol.* **1985**, *38*, 87.
[47] H. Mühlpfort, *Experimenta* **1982**, *38*, 1127.
[48] P. Mukherjee, A. Ahmad, D. Mandal, S. Senapati, S. R. Sainkar, M. I. Khan, R. Ramans, R. Parisaka, P. V. Ajayakumar, M. Alam, M. Sastry, R. Kumar, *Angew. Chem. Int. Ed.* **2001**, *40*, 3585.
[49] G. Schmid, A. Lehnert, J.-O. Malm, J.-O. Bovin, *Angew. Chem.* **1991**, *103*, 852; *Angew. Chem. Int. Ed. Engl.* **1991**, *30*, 874.
[50] Ch. J. Baddeley, D. A. Jefferson, R. M. Lambert, R. M. Ormerod, T. Rayment, G. Schmid, A. P. Walker, *Mat. Res. Soc., Symp. Proc.* Vol. 272, 1992 Materials Research Society.
[51] G. Schmid, R. Pugin, Th. Sawitowski, U. Simon, B. Marler, *Chem. Commun.* **1999**, 1303.
[52] M. C. Fairbanks, R. E. Benfield, R. J. Newport, G. Schmid, *Solid State Commun.* **1990**, *73*, 431.
[53] P. D. Cluskey, R. J. Newport, R. E. Benfield, S. J. Gurmann, G. Schmid, *Z. Phys. D* **1993**, *26*, 8.
[54] R. C. Thiel, R. E. Benfield, R. Zanoni, H. H. A. Smit, M. W. Dirken, *Z. Phys. D* **1993**, *81*, 1.
[55] H. H. A. Smit, R. C. Thiel, L. J. de Jongh, *Z. Phys. D* **1989**, *12*, 193.
[56] J. W. A. van der Velden, F. A. Vollenbroek, J. J. Bour, P. I. Beurskens, J. M. M. Smits, W. P. Bosman, *Recl.: J. R. Neth. Chem. Soc.* **1981**, *100*, 148.
[57] C. E. Briant, B. R. C. Theobald, J. W. White, C. K. Bell, D. M. P. Mingos, *J. Chem. Soc., Chem. Commun.* **1981**, 201.
[58] B. K. Teo, X. Shi, H. Zhang, *J. Am. Chem. Soc.* **1992**, *114*, 2743.
[59] T. Sawitowski, Y. Miquel, A. Heilmann, G. Schmid, *Adv. Funct. Mater.* **2001**, *11*, 435.
[60] G. L. Hornyak, M. Kröll, R. Pugin, Th. Sawitowski, G. Schmid, J.-O. Bovin, G. Karsson, H. Hofmeister, S. Hopfe, *Chem. Eur. J.* **1997**, *3*, 1951.
[61] *Optical Properties of Metal Clusters* (Eds.: U. Kreibig, M. Vollmer), Springer, Berlin 1995.
[62] D. Schönauer, M. Quinten, U. Kreibig, *Z. Phys. D* **1989**, *12*, 527.
[63] M. Quinten, U. Kreibig, *Appl. Opt.* **1993**, *32*, 6173.
[64] M. Herrmann, U. Kreibig, G. Schmid, *Z. Phys. D* **1993**, *26*, 1.
[65] B. A. Smith, J. Z. Zhang, U. Giebel, G. Schmid, *Chem. Phys. Lett.* **1997**, *270*, 139.
[66] A. Bezryadin, C. Dekker, G. Schmid, *Appl. Phys. Lett.* **1997**, *71*, 1273.
[67] L. F. Chi, M. Hartig, T. Drechsler, Th. Schwaack, C. Seidel, H. Fuchs, G. Schmid, *Appl. Phys. A* **1998**, *66*, 187.
[68] H. Zhang, G. Schmid, U. Hartmann, *Nano Lett.* **2003**, *3*, 305.
[69] V. Torma, O. Vidoni, U. Simon, G. Schmid, *Eur. J. Inorg. Chem.* **2003**, 1121.
[70] G. Schmid, M. Bäumle, N. Beyer, *Angew. Chem.* **2000**, *112*, 187−189; *Angew. Chem. Int. Ed.* **2000**, *39*, 181.
[71] G. Schmid, N. Beyer, *Eur. J. Inorg. Chem.* **2000**, 835.
[72] Th. Sawitowski, St. Franzka, N. Beyer, M. Levering, G. Schmid, *Adv. Funct. Mater.* **2001**, *11*, 169.
[73] V. Torma, T. Reuter, O. Vidoni, M. Schumann, C. Radehaus, G. Schmid, *ChemPhysChem.* **2001**, *8/9*, 546.
[74] S. Liou, R. Maoz, G. Schmid, J. Sagiv, *Nano Lett.* **2002**, *2*, 1055.
[75] G. Schmid, "The Way to Large Clusters", *Struct. Bonding* **1985**, *62*, 51.

[76] G. Schmid, W. Meyer-Zaika, R. Pugin, T. Sawitowski, J.-P. Majoral, A.-M. Caminade, C.-O. Turrin, *Chem. Eur. J.* **2000**, *6*, 1693.
[77] H.-G. Boyen, G. Kästle, F. Weigl, B. Koslowski, C. Dietrich, P. Ziemann, J. P. Spatz, S. Riethmüller, C. Hartmann, M. Möller, G. Schmid, M. G. Garnier, P. Oelhafen, *Science* **2002**, *297*, 1533.
[78] *Chem. Eng. News* **2002**, *80*, p. 29.
[79] *Catalyst Handbook* (Ed.: M. V. Twigg), Manson, 1996.
[80] G. C. Bond, D. T. Thomson, *Catal. Rev. Sci. Eng.* **1999**, *41*, 319.
[81] G. C. Bond, *Catal. Today* **2002**, *72*, 5.
[82] W. A. Bone, R. V. Wheeler, *Trans. Royal Chem. Soc., A* **1906**, *206*, 1.
[83] G. C. Bond, *Gold Bull.* **1971**, *5*, 11.
[84] G. C. Bond, P. A. Sermon, *Gold Bull.* **1973**, *6*, 102.
[85] S. Galvagno, G. Parravano, *J. Catal.* **1978**, *55*, 178.
[86] D. McIntosh, G. A. Ozin, *Inorg. Chem.* **1976**, *15*, 2689.
[87] D. McIntosh, G. A. Ozin, *Inorg. Chem.* **1977**, *16*, 51.
[88] T. V. Choudary, D. W. Goodman, *Top. Catal.* **2002**, *21*, 25.
[89] M. Haruta, N. Yamada, T. Kobayashi, S. Lijima, *J. Catal.* **1989**, *115*, 301.
[90] M. Haruta, S. Tsuboda, T. Kobayashi, H. Kagehiama, M. J. Genet, B. Delmon, *J. Catal.* **1993**, *144*, 175.
[91] G. Schmid, *J. Chem. Soc., Dalton Trans.* **1998**, 1077.
[92] M. Valden, X. Lai, D. W. Goodman, *Science* **1998**, *281*, 1647.
[93] G. C. Bond, D. T. Thomson, *Gold Bull.* **2000**, *33*, 41.
[94] G. C. Bond, D. T. Thomson, *Catal. Rev.-Sci. Eng.* **1999**, *41*, 319.
[95] A. Wolf, F. Schüth, *Appl. Catal., A* **2002**, *226*, 1.
[96] M. Haruta, *Catal. Today* **1997**, *36*, 153.
[97] S. Schimpf, M. Lucas, C. Mohr, U. Rodemerk, A. Brückner, J. Radnik, H. Hofmeister, P. Claus, *Catal. Today* **2002**, *72*, 63.
[98] A. Zwijnenburg, M. Saleh, M. Makker, J. A. Moulijn, *Catal. Today* **2002**, *72*, 59.
[99] M. Haruta, *CATTECH* **2002**, *6*, 102.
[100] M. Daté, Y. Ichihashi, T. Yamashita, A. Chiorino, F. Boccuzzi, M. Haruta, *Catal. Today* **2002**, *72*, 89.
[101] T. Akita, P. Lu, S. Ichikawa, K. Tanaka, M. Haruta, *Surf. Interface Anal.* **2001**, *31*, 73.
[102] B. Corain, D. Ferrari, P. Centomo, S. Lora, W. Mayer-Zaika, G. Schmid, manuscript in preparation.
[103] F. Porta, L. Prati, M. Rossi, S. Coluccia, G. Martra, *Catal. Today* **2000**, *61*, 165.
[104] J.-D. Grunwaldt, C. Kiener, C. Wögerbauer, A. Baiker, *J. Catal.* **1999**, *181*, 223.
[105] W. T. Wallace, R. L. Whetten, *J. Am. Chem. Soc.* **2002**, *124*, 7499.
[106] N. Lopez, J. K. Norskov, *J. Am. Chem. Soc.* **2002**, *124*, 11262.
[107] R. Grisel, K.-J. Westrate, A. Gluhoi, B. Niewenhuis, *Gold Bull.* **2002**, *35*, 39.
[108] M. Okumura, S. Nakamura, S. Tsubota, T. Nakamura, M. Azuma, *Catal. Lett.* **1998**, *51*, 53.
[109] M. Okumura, T. Akita, M. Haruta, *Catal. Today* **2002**, *74*, 265.
[110] C. Mohr, H. Hofmeister, P. Claus, *J. Catal.* **2003**, *213*, 86.
[111] S. Biella, M. Rossi, *Chem. Commun.* **2003**, 378.
[112] S. Minicò, S. Sciré, C. Crisafulli, R. Maggiore, S. Galvagno, *Appl. Catal., B* **2000**, *28*, 245.
[113] C. Milone, R. Ingoglia, G. Neri, A. Pistone, S. Galvagno, *Appl. Catal., A* **2001**, *211*, 251.
[114] S. Biella, G. L. Castiglioni, C. Fumagalli, L. Prati, M. Rossi, *Catal. Today* **2002**, *72*, 43.
[115] C. Milone, M. L. Tropeano, G. Gulino, G. Neri, R. Ingoglia, S. Galvagno, *Chem. Commun.* **2002**, 868.
[116] C. Milone, R. Ingoglia, M. L. Tropeano, G. Neri, G. Galvagno, *Chem. Commun.* **2003**, 868.
[117] P. Landon, P. J. Collier, A. J. Papworth, C. J. Kiely, G. J. Hutchings, *Chem. Commun.* **2002**, 2058.
[118] F. Shi, Y. Deng, *J. Catal.* **2002**, *211*, 548.
[119] C. W. Corti, R. J. Holliday, D. T. Thomson, *Gold Bull.* **2002**, *35*, 11.

Received April 3, 2003

